Nanotechnology **19** (2008) 384018 (6pp) doi:10.1088/0957-4484/19/38/384018

High-speed AFM of human chromosomes in liquid

L M Picco[1], P G Dunton[1], A Ulcinas[1], D J Engledew[1], O Hoshi[2], T Ushiki[2] and M J Miles[1]

[1] H H Wills Physics Laboratory and IRC in Nanotechnology, University of Bristol, Tyndall Avenue, Bristol BS8 1TL, UK
[2] Division of Microscopic Anatomy and Bio-Imaging, Department of Cellular Function, Niigata University Graduate School of Medical and Dental Sciences, Asahimachi-Dori 1, Niigata, 951-8150, Japan

E-mail: m.j.miles@bristol.ac.uk

Received 23 June 2008
Published 12 August 2008
Online at stacks.iop.org/Nano/19/384018

Abstract
Further developments of the previously reported high-speed contact-mode AFM are described. The technique is applied to the imaging of human chromosomes at video rate both in air and in water. These are the largest structures to have been imaged with high-speed AFM and the first imaging in liquid to be reported. A possible mechanism that allows such high-speed contact-mode imaging without significant damage to the sample is discussed in the context of the velocity dependence of the measured lateral force on the AFM tip.

(Some figures in this article are in colour only in the electronic version)

1. Introduction

The advantages of atomic force microscopy (AFM) (Binnig *et al* 1986) for imaging biological samples are well known. Of particular importance for biology is the ability of AFM to image at high resolution in an aqueous environment, thus allowing the possibility that a biomolecular sample may be functionally active during observation. However, conventional AFM operated in its most common modes—contact, non-contact and intermittent contact—has the major disadvantage of a low imaging rate, requiring typically a minute or more to acquire an image, depending on the image area and sample roughness. This limitation arises from the fact that AFM is a mechanical microscope in both the sample scan method and the detection of the sample surface through the bending of a microcantilever, and consequently is subject to inertial and resonance limitations.

The most direct approach to overcoming these limitations imposed by the mechanics of the AFM is to reduce the mass and increase the resonant frequencies of both the scanner and the cantilever. This has the effect of shifting the time domain to shorter timescales, allowing faster imaging. With higher imaging speeds, it is, of course, necessary to increase the speed of the feedback loop (electronic and mechanical) and the bandwidth of the data capture electronics. The pioneers of this approach have been the Hansma (Viani *et al* 2000, Fantner *et al* 2005) and Ando (Sakamoto *et al* 2000, Ando *et al* 2006) groups and others (Schitter *et al* 2004, Rost *et al* 2005) using smaller cantilevers (∼7μm long) with higher resonant frequencies (∼1 MHz). This small-cantilever tapping-mode version of high-speed imaging has been particularly successful in imaging individual biomolecules and their associated bioprocesses.

An alternative approach to high-speed (HS) SPM has been taken in Bristol, initially based around a resonant scanning system: first, for scanning near-field optical microscopy (Humphris *et al* 2003) and then for AFM (Humphris *et al* 2005). In the case of the latter, the method involves contact-mode imaging in which the tip is scanned at high-speed relative to the sample and a conventional AFM feedback system, with a response time of about 1 ms, maintains on average a constant force but is unable to correct the tip position with pixel resolution. Topographic information is obtained through the deflection of the cantilever determined using either an optical lever or interferometer. Contrary to expectations, such high imaging speeds in contact mode without correspondingly fast feedback do not produce significant damage to most specimens even after thousands of images have been collected. This contact-mode high-speed AFM has particular advantages over the small-cantilever tapping-mode method for scanning

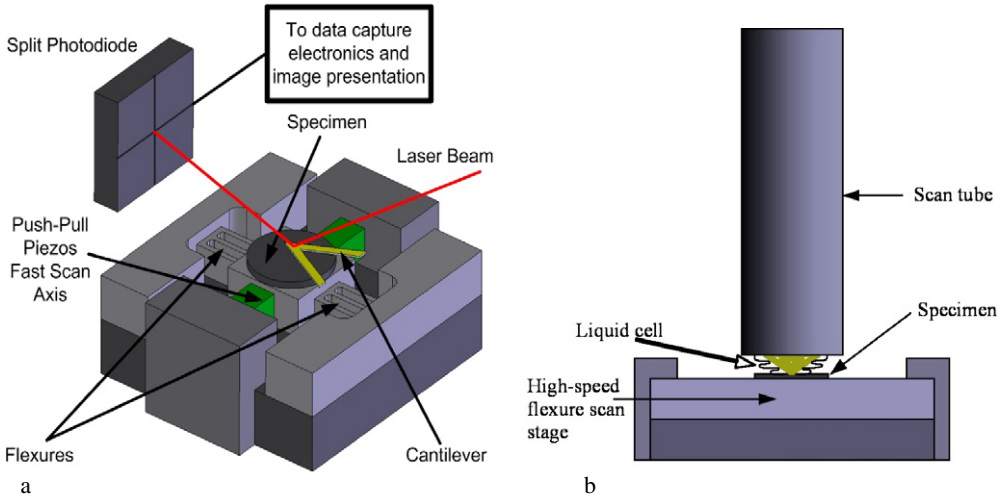

Figure 1. (a) A schematic diagram of the high-speed flexure scanning stage in relation to the microcantilever; (b) the scan tube and liquid cell in relation to the cantilever and flexure stage.

larger sample areas with greater height variations. HS AFM has also achieved the highest AFM imaging rates with over 1000 frames s^{-1} being reported on biomolecular samples (Picco *et al* 2007).

2. Experimental details

2.1. High-speed AFM instrumentation

A high-speed scanning system based on a flexure stage, constructed in-house, was employed for video rate imaging in both air and liquid. The high-speed system was mounted on a Veeco Dimension 3100 such that conventional AFM could also be performed. In conventional and high-speed AFM, the fast scan direction (x) was set as the horizontal direction in the image and the slow scan as the vertical direction (y). The cantilever was mounted on the scan tube with its long axis aligned with the slow scan direction (see figure 1(a)). The scan tube also provided the z-direction control used to maintain on average a constant preset cantilever deflection. During HS imaging the frame scan was driven by a triangular voltage waveform. The line scan, however, was created from a sinusoidal waveform; this serves to prevent the introduction of higher-order vibrational modes into the fast scan direction (Rost *et al* 2005). The displayed images are easily corrected in real time to account for the nonlinear tip velocities. A sine wave was also used to drive the x axis when taking measurements of the velocity dependence of the lateral forces on the tip.

The cantilevers used were supplied by Veeco (Santa Barbara, CA). Cantilever bending was measured by the optical lever method (Alexander *et al* 1989). Deflection data were captured and image construction performed in real time using in-house-designed National Instruments LabView software. The bending and torsional displacement of the cantilever were detected by a quadrant photodiode. The bending signal was used for image formation and the torsional signal was used to investigate the dependence of the frictional and viscous lateral forces on the tip as a function of tip–sample velocity, in order to gain an insight into the origin of the unexpectedly low damage to the sample at high velocities.

2.2. Human chromosome preparation

Human lymphocytes were taken from heparinized peripheral blood of healthy donors and were cultivated in a karyotyping medium (PB-max, Gibco, Invitrogen Co, Carlsbad) with 10% foetal calf serum for 72 h at 37 °C under 5% CO_2 and 95% air. Colcemid was added to the culture medium at a final concentration of 0.05 $\mu g\,ml^{-1}$ for 1 h, resulting in arrest of lymphocytes in metaphase. The suspension of cells was then exposed for 30 min at room temperature to 75 mM KCl and fixed with an acetic acid and methanol mixture (1:3). Chromosome spreads were prepared by dropping the cell suspension onto glass coverslips, followed by air-drying in a humid condition for 10 min.

3. Results and discussion

Sets of human metaphase chromosomes spread on glass coverslips were examined with both conventional AFM and HS AFM. Figure 2(a) shows a contact-mode image of a set of human chromosomes imaged in air with conventional AFM with standard feedback electronics and software. Particular metaphase chromosomes can be identified by their size and the ratio of the lengths of their chromatid arms, and are numbered beginning with the longest. In this dry state, the height of the chromosomes is around 80 nm. High-speed AFM imaging in air of such a set of chromosomes resulted in a sequence of images taken at a video rate of 30 frames s^{-1}. Several of these images from neighbouring regions can be assembled into a montage such as that shown in figure 3.

It is remarkable that objects as tall as this can be imaged repeatedly with no significant damage using a method in which the feedback used is essentially that of a conventional AFM and so too slow to reposition the tip above the sample at high

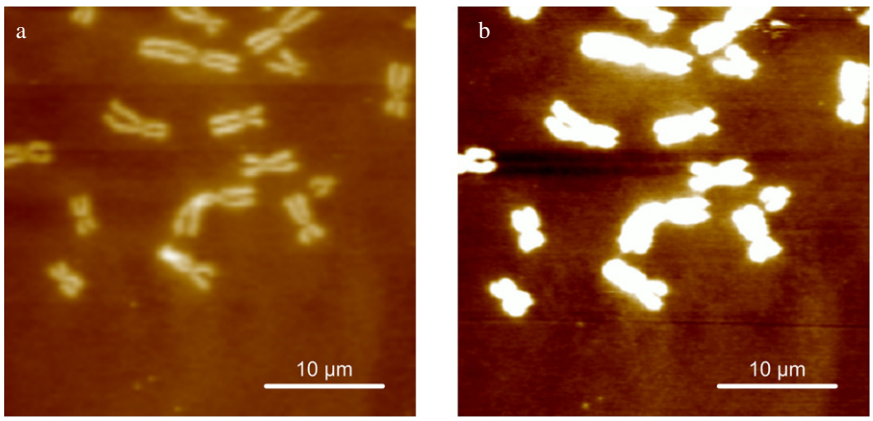

Figure 2. Conventional contact-mode images of a set of human chromosomes (a) in air and (b) in 2 mM NaCl buffer. Image size: 36 μm $\times$ 36 μm; height range: 250 nm.

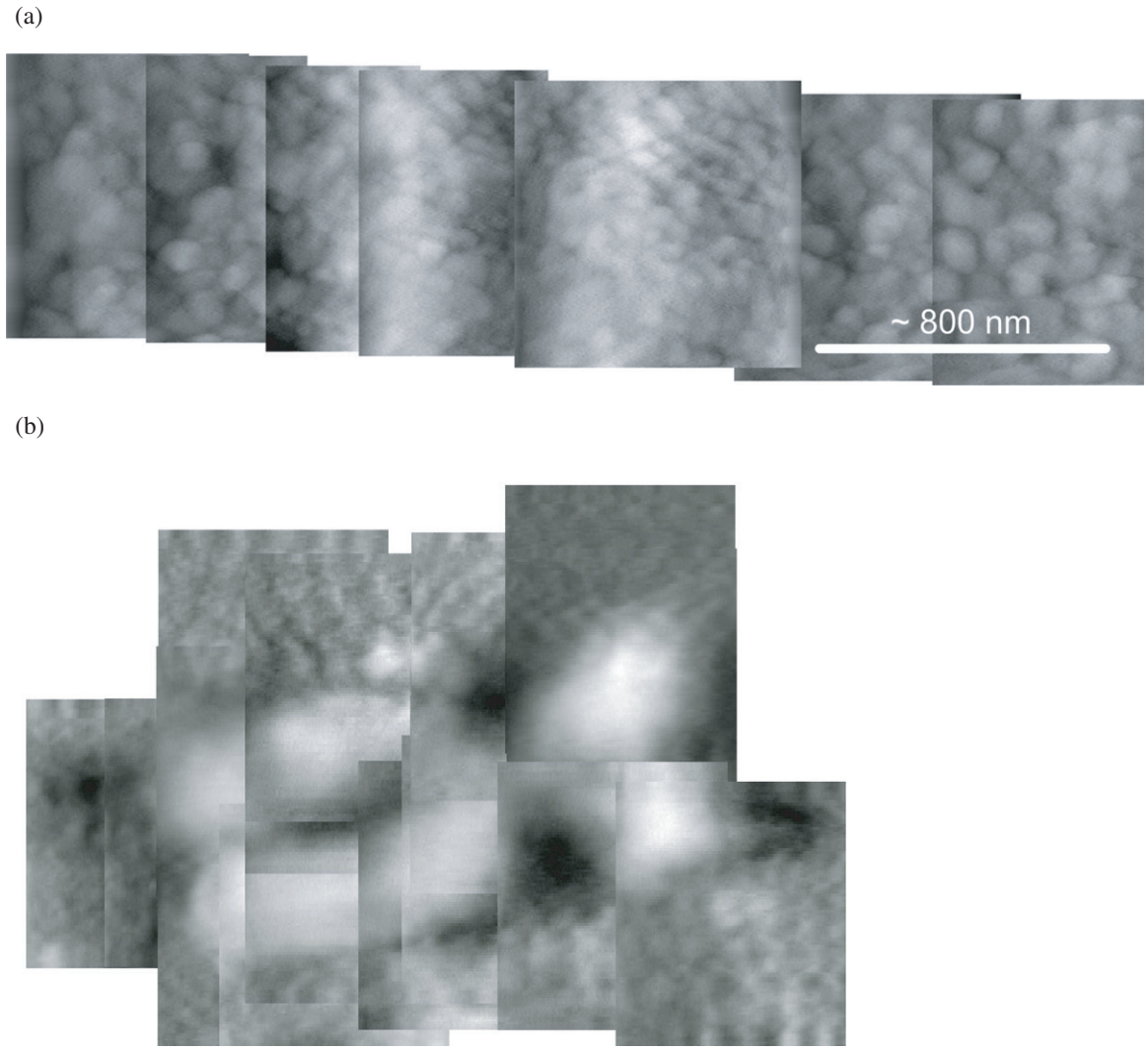

Figure 3. (a) Montage of HS AFM chromosome images (a) passing over the ends of two chromatids (the histone structures covering the chromatids are observed at this scale) and (b) showing the entirety of a metaphase chromosome.

speed in order to minimize the force imposed. One possible explanation for samples which exhibit significant viscoelastic behaviour is that the sample deformation rates associated with the high velocity of the AFM tip result in a greater sample stiffness at the higher shear rates associated with the speed of imaging. This is a particularly relevant argument in the

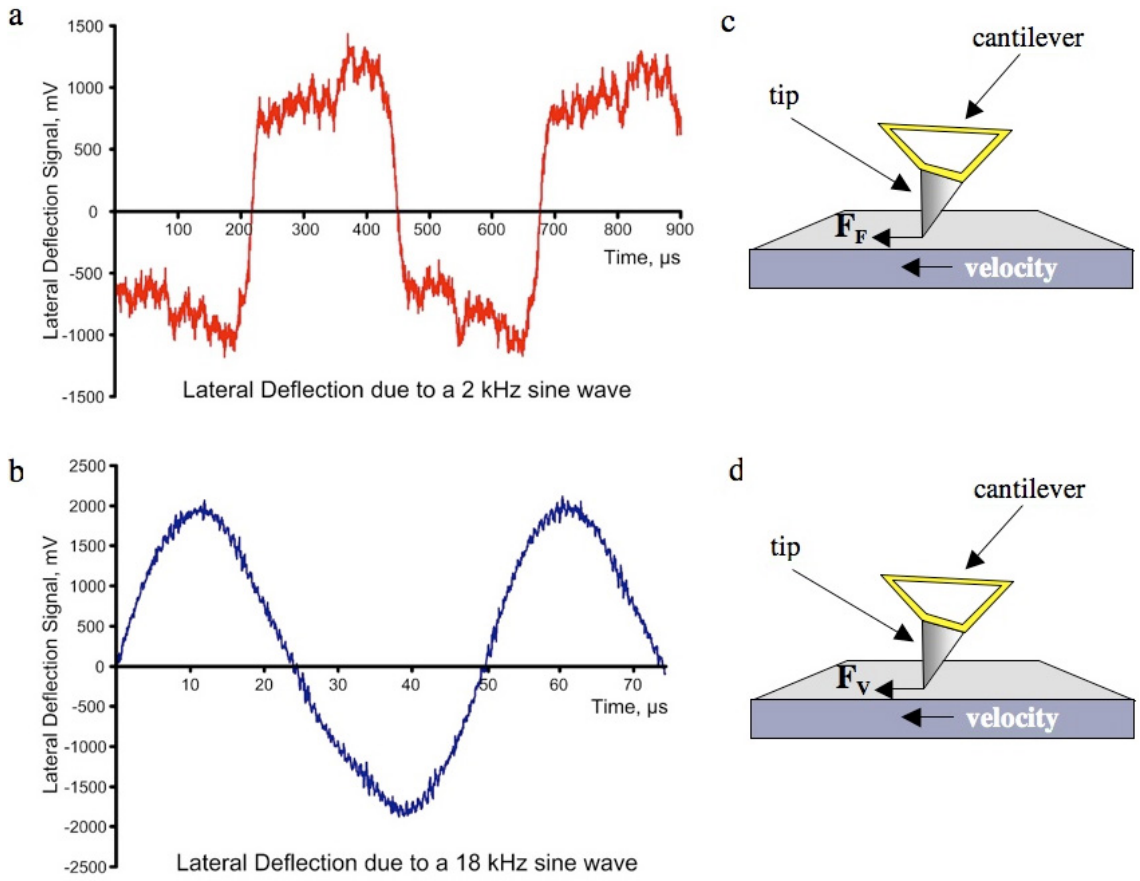

Figure 4. A mica sample was oscillated sinusoidally with amplitude 0.5 μm at a frequency of (a) 2 kHz and (b) 18 kHz. The lateral deflection signal from the cantilever was recorded in both cases. At the lower frequency and corresponding lower velocity in (a), the lateral deflection signal showed an almost constant force which depended only on the sign of the velocity but was independent of its value over the range of the applied sine wave displacement. A frictional force between the tip and specimen (as indicated in (c)) can explain this observation. At the higher frequency and velocity in (b), the lateral deflection signal is sinusoidal, corresponding to the sinusoidal velocity of the sample. This can be explained by a viscous force (as indicated in (d)) as the tip moves through an adsorbed water layer.

case where the sample is a polymer and, to some extent, is applicable to the chromosome samples investigated here. However, our recent measurements of the velocity dependence of the lateral force on the tip indicate that other mechanisms may play an important role at high tip–sample velocities.

Figure 4 shows the dependence of lateral force on the relative tip–sample velocity. The sample in this case is a cleaved mica surface. The sample is being oscillated laterally in a sinusoidal motion and the torsional bending of the cantilever is recorded in the configuration shown in figure 1. The conventional AFM feedback maintains a constant force with a response time of about 1 ms. At low speeds, where the average relative velocity during one sinusoidal cycle is about 2 mm s^{-1}, the lateral force exerted on the tip was found to having an approximately square-wave dependence on time despite the velocity of the probe being sinusoidal with time. As the tip moves in one direction, the torsion remains approximately constant but with a slope which is the result of the sample presenting a sloping surface with respect to the plane of motion of the tip. When the tip turns around at the end of the scan line, the torsion was observed to have the opposite sign but again showing a square-like response with a superimposed sample slope. This behaviour is consistent with the torque on the cantilever and the force on the end of the tip being approximately constant for a given direction of tip–sample motion. This requires a force that is not velocity-dependent and suggests that the frictional force between the tip and sample is the major factor causing the torsional rotation of the cantilever at speeds up to 2 mm s^{-1}. Figure 4(c) illustrates this situation.

At higher tip–sample velocities such as the 20 mm s^{-1} used for the data of figure 4(b), the cantilever torsion was found to be sinusoidal in time, such that the maxima and minima of the sine wave corresponded to the maxima and minima in the tip velocity. This velocity dependence is not consistent with a constant force associated with tip–sample friction, but rather suggests a force arising from viscosity of a fluid. Under ambient conditions, a thin film of adsorbed water exists on hydrophilic surfaces. It can therefore be inferred that this fluid layer imposes viscous drag forces at the end of the tip and causes the velocity-dependent torsion of the cantilever. The fact that the square-wave dependence is no longer evident suggests that the tip and sample are no longer in direct contact. One explanation is that the velocity of the tip through the water layer generates a hydrostatic pressure which results in the tip lifting off the sample surface,

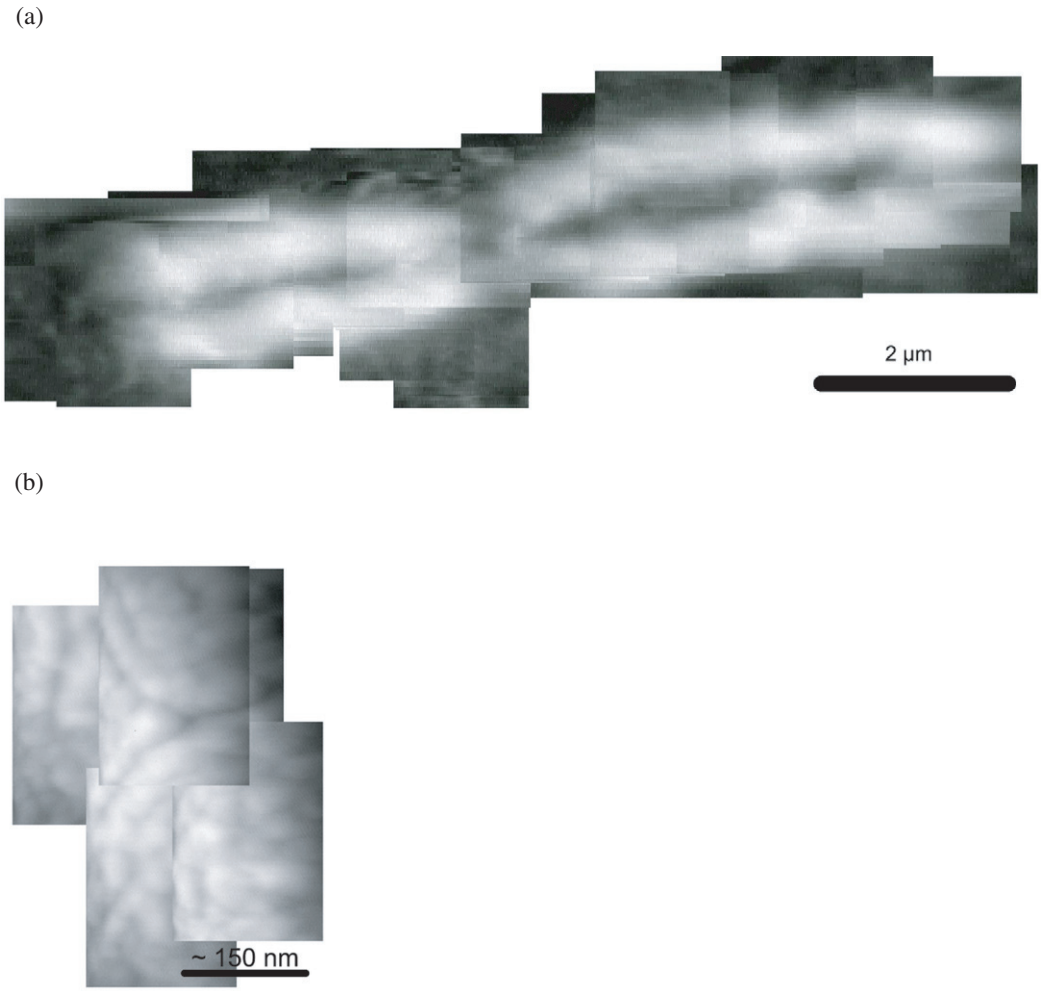

Figure 5. High-speed AFM images collected at a frame rate of 20 frames/s in water where (a) is a montage of images showing chromosome 2 and (b) is a higher-resolution image of the top of a chromosome (chromosome 2) showing chromatin structures.

thus removing the surface friction component of the force on the tip (Skotheim and Mahadevan 2005). This mechanism (sometimes known as superlubricity) provides an automatic feedback, since, with increasing tip–sample separation the hydrostatic pressure produced will decrease. Thus, for a given tip and velocity an equilibrium tip–sample separation distance will be attained. An additional possibility is that at high velocities the slip length may change and this is also velocity-dependent (Thompson and Trolan 1997). For both of these cases, the result is lower shear forces applied to the sample by the tip and thus provides an explanation for the considerably reduced sample distortion and damage observed at these speeds.

Figure 2(b) shows a conventional contact-mode AFM image of a set of hydrated human chromosomes recorded in water. Note that the height scale of figures 2(a) and (b) is the same, emphasizing the dramatic height increase. In the aqueous environment, the chromosomes have swollen by a factor of five in height such that they are sometimes over 500 nm thick. This also indicates that the hydrated chromosomes have softened considerably as compared with dried specimens. Figure 5(a) shows a composite image of a metaphase chromosome (chromosome 2) created from a series of HS AFM images collected at 30 frames s^{-1} in water. It was possible to move around the sample in real time, as might be done with a conventional optical microscope, and image different chromosomes. From such a movie, larger scale montages can be constructed. A comparison of the observed structure from the HS AFM with conventional AFM indicates that similar variations in height and width along the length of the chromatids are seen (Hoshi *et al* 2004). Figure 5(b) shows a higher-magnification HS AFM image of the top surface of one chromatid in water. These images have sufficient resolution to show structures on the surface such as chromatin structures (Ushiki and Hoshi 2008) and it is possible to move along the length of the chromosome, imaging continuously.

Extension of high-speed contact-mode AFM imaging to the liquid environment opens up many possibilities not accessible to imaging in air alone. These are the first reported images of this HS contact AFM technique imaging a biological specimen in liquid. The observation that high-speed contact-mode AFM was possible was in itself unexpected and some possible explanations for this phenomenon are set out above and further experimental and theoretical studies are

obviously required. However, the extension of this technique to the imaging of large and soft objects such as hydrated chromosomes requires a further explanation regarding the behaviour of the cantilever in responding to such large and rapid height changes at frequencies greater than its fundamental resonant frequency. In this mode, the cantilever should respond as a rigid body but this cannot be the case as the imaging signal is the deflection arising from the bending of the cantilever at the tip end. An explanation could be that the cantilever is responding to these higher frequencies through bending in higher modes that correspond to the higher harmonics of the cantilever. Damping of the cantilever in liquid will cause broadening of all harmonics and avoids resonance artefacts in the images.

4. Conclusions

High-speed AFM imaging of human chromosomes both in air and in liquid has been achieved. These structures are the largest both in height as well as in lateral dimensions so far imaged at high speed and the first time that imaging in liquid with this technique has been reported. The spatial resolution achieved was found to be similar to that of AFM at conventional speeds on similar samples. It is clear that it is very important to understand better the mechanics of the cantilever and the interaction of the tip with the sample at these high speeds and frequencies, not least to optimize the imaging conditions and to design and fabricate cantilevers to take advantage of this understanding, thereby improving the performance of this technique in respect of the forces applied, the resolution achieved and the imaging rates attainable.

Acknowledgments

LMP and DJE are supported by the IRC in Nanotechnology (EPSRC). PGD is funded by the EU project 'Tips4Cells' (LSGH-CT-2005-512101). OH and TU are supported by GASR (no. 18390058) from the JSPS, Japan.

References

Alexander S, Hellemans L, Marti O, Schneir J, Elings V, Hansma P, Longmire M and Gurley J 1989 An atomic-resolution atomic force microscope implemented using an optical lever *J. Appl. Phys.* **65** 164–7

Ando T *et al* 2006 High-speed atomic force microscopy for studying the dynamic behavior of protein molecules at work *Japan J. Appl. Phys.* 1 **45** 1897–903

Binnig G, Quate C F and Gerber C 1986 Atomic force microscope *Phys. Rev. Lett.* **56** 930–3

Fantner G E, Hegarty P, Kindt J H, Schitter G, Cidade G A G and Hansma P K 2005 Data acquisition system for high speed atomic force microscopy *Rev. Sci. Instrum.* **76** 026118

Hoshi O, Owen R, Miles M and Ushiki T 2004 Imaging of human metaphase chromosomes by atomic force microscopy in liquid *Cytogenet. Genome Res.* **107** 28–31

Humphris A D L, Hobbs J K and Miles M J 2003 Ultrahigh-speed scanning near-field optical microscopy capable of over 100 frames per second *Appl. Phys. Lett.* **83** 6–8

Humphris A D L, Miles M J and Hobbs J K 2005 A mechanical microscope: High-speed atomic force microscopy *Appl. Phys. Lett.* **86** 034106

Picco L M, Bozec L, Ulcinas A, Engledew D J, Antognozzi M, Horton M A and Miles M J 2007 Breaking the speed limit with atomic force microscopy *Nanotechnology* **18** 044030

Rost M J *et al* 2005 Scanning probe microscopes go video rate and beyond *Rev. Sci. Instrum.* **76** 053710

Sakamoto T, Amitani I, Yokota E and Ando T 2000 Direct observation of processive movement by individual myosin V molecules *Biochem. Biophys. Res. Commun.* **272** 586–90

Schitter G, Allgower F and Stemmer A 2004 A new control strategy for high-speed atomic force microscopy *Nanotechnology* **15** 108–14

Skotheim J M and Mahadevan L 2005 Soft lubrication: The elastohydrodynamics of nonconforming and conforming contacts *Phys. Fluids* **17** 092101–23

Thompson P A and Trolan S M 1997 A general boundary condition for liquid flow at a solid surface *Nature* **389** 360–2

Ushiki T and Hoshi O 2008 Atomic force microscopy for imaging human metaphase chromosomes *Chromosome Res.* **16** 383–96

Viani M B, Pietrasanta L I, Thompson J B, Chand A, Gebeshuber I C, Kindt J H, Richter M, Hansma H G and Hansma P K 2000 Probing protein-protein interactions in real time *Nat. Struct. Biol.* **7** 644–7